Supplementary Material for "Prediction of room temperature antiferromagnetism in V_2CT_2 (T = Cl, Br, I) MXenes"

by Kan Luo, Xianghua Kong, Shiyu Du and Hong Guo

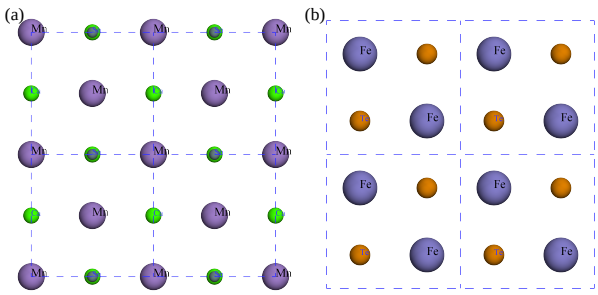

FIG. S1: Top-view representations of the geometric structures for MnCaSn (a) and FeTe (b).

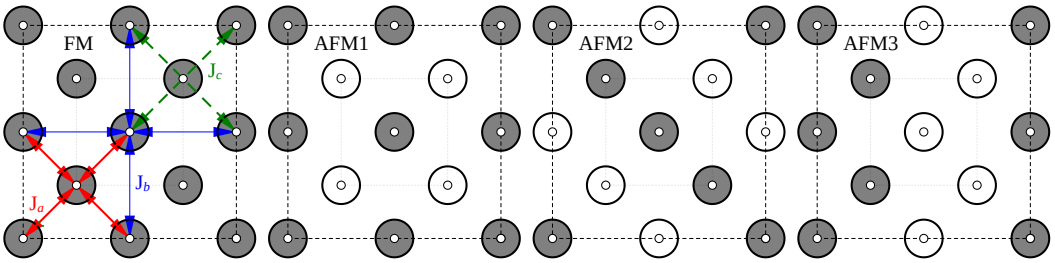

FIG. S2: The FM and AFM configurations for square lattice. Black and white circles represent spin-up and spin-down, respectively.

TABLE S1: The calculated relative energy per formula unit for MnCaSn and FeTe. The relative energy for the AFM1 configuration is set to zero and highlighted in bold.

(meV)	ICSD	FM	AFM1	AFM2	AFM3	J_a	J_b	J_c	A	T_c
MnCaSn	66958	95.31	**0.0**	37.56	59.02	−23.828	−2.525	4.105	0.298	235
FeTe	180602	178.70	**0.0**	15.69	81.87	−44.675	−18.415	7.337	0.203	240

Just take the up and down spins into account, the possible spin states for 2D square lattice can be divided into four major types (one FM and three AFMs). FM state intends all spins point to the same direction, while AFM state means an equivalent number of spins with opposite alignment in sublattices could be found and exhibit zero magnetization. A supercell containing 8 magnetic atoms forming four possible magnetic arrangements in a square lattice is illustrated in Fig. S2, where the black and white circles represent spin-up and spin-down states, respectively. J_a, J_b and J_c denote the intralayer exchange coupling interactions between the nearest, next-nearest, and third-nearest neighbors, as depicted in Fig. 1. The total energies for FM and AFMs 1–3 can be expressed as Eq. (S1), and J_a, J_b and J_c are then expressed in Eq. (S2).

$$\begin{aligned} E_{FM} &= E_0 - 2J_aS^2 - 2J_bS^2 - 2J_cS^2, \\ E_{AFM1} &= E_0 + 2J_aS^2 - 2J_bS^2 - 2J_cS^2, \\ E_{AFM2} &= E_0 + 2J_bS^2 - 2J_cS^2, \\ E_{AFM3} &= E_0 + 2J_cS^2. \end{aligned} \tag{S1}$$

Supplementary Material for "Prediction of room temperature antiferromagnetism in V_2CT_2 (T = Cl, Br, I) MXenes"

by Kan Luo, Xianghua Kong, Shiyu Du and Hong Guo

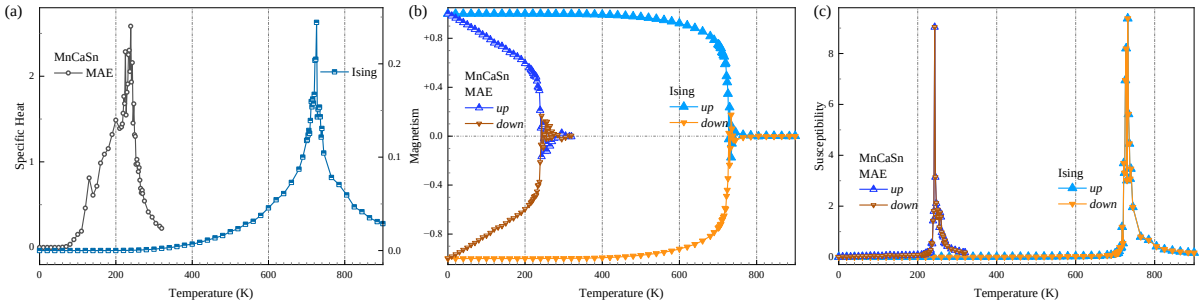

FIG. S3: Temperature-dependent changes in specific heat (a), magnetic properties (b), and susceptibility (c) for MnCaSn monolayer, with and without consideration of MAE, respectively.

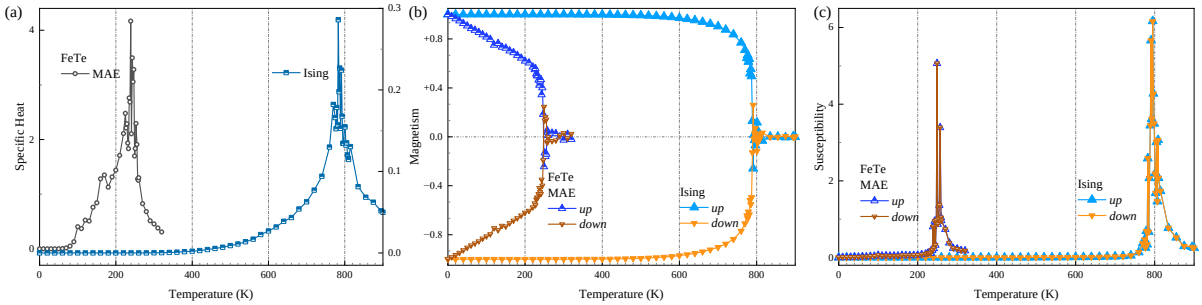

FIG. S4: Temperature-dependent changes in specific heat (a), magnetic properties (b), and susceptibility (c) for FeTe monolayer, with and without consideration of MAE, respectively.

$$\begin{aligned} J_a &= \frac{E_{AFM1} - E_{FM}}{4S^2}, \\ J_b &= \frac{E_{AFM2} - E_{AFM1}}{4S^2} + \frac{J_a}{2}, \\ J_c &= \frac{E_{AFM3} - E_{AFM2}}{4S^2} + \frac{J_b}{2}. \end{aligned} \tag{S2}$$

$$\begin{aligned} k_B T_c^{(3)} &= \frac{2}{\ln(2+\sqrt{3})} J, T_c^{(3)} \approx 1.519 J/k_B \\ k_B T_c^{(4)} &= \frac{2}{\ln(1+\sqrt{2})} J, T_c^{(4)} \approx 2.269 J/k_B \\ k_B T_c^{(6)} &= \frac{4}{\ln(3)} J \qquad , T_c^{(6)} \approx 3.641 J/k_B \end{aligned} \tag{S3}$$

$$\boldsymbol{p} = \frac{1}{\sqrt{x^2+y^2+z^2}} \begin{bmatrix} x \\ y \\ z \end{bmatrix} \tag{S4}$$

The analytical solutions of honeycomb, square and triangular lattices are provided in Eq. (S3), where the number in the upper right corner indicates the nearest neighbor coordination number, k_B is the Boltzmann constant and J is the nearest-neighbor coupling.

New state obtained by normalizing three independent Gaussian random variable x, y and z as described in Eq. (S4), to ensure that the possibility $\boldsymbol{p}$ is uniformly distributed over the sphere.

Following is an example of generating a random, uniformly distributed arrange over the sphere.

```
def NormalrandNN(n, m, Y, X):
  arr = np.zeros((n, m, Y, X, 3)).astype(np.float32)
  for i in range(n):
  for j in range(m):
  arr_t = np.random.randn(3, X, Y)
  arr_t = arr_t / np.sqrt(arr_t[0]**2 + arr_t[1]**2 + arr_t[2]**2)
  arr[i,j] = arr_t.T
return arr
```

The probability to accept the new state using Metropolis–Hastings algorithm is given by Eq. (S5).

$$A(\alpha \to \beta) = \begin{cases} 1 & , E_\alpha \geq E_\beta \\ exp(-\dfrac{E_\beta - E_\alpha}{k_B T}), & E_\beta < E_\alpha \end{cases} \tag{S5}$$

The mean magnetization $\langle m \rangle$, magnetic susceptibility χ and specific heat c per spin are obtained through statistics analysis and are defined in Eq. (S6), where N denotes the total number of magnetic atoms and T is the temperature.

$$\begin{aligned} \langle m \rangle &= \frac{1}{N} \sum_i^N \mathbf{S}_i \\ \chi &= \frac{N}{k_B T} (\langle m^2 \rangle - \langle m \rangle^2) \\ c &= \frac{1}{k_B T^2 N} (\langle E^2 \rangle - \langle E \rangle^2) \end{aligned} \tag{S6}$$

Additionally, only the sign (1 or -1) of the contributions along the easy axis is considered in the specific heat calculation within the Heisenberg model, to improve the accuracy in identifying the critical temperature T_c.

TABLE S2: The optimized lattice parameters a and b for V_2CT_2 (T = F, Cl, Br, I).

(Å)	V_2CF_2	V_2CCl_2	V_2CBr_2	V_2CI_2
a	3.171	3.348	3.447	3.620
b	5.291	5.600	5.781	6.092

Supplementary Material for "Prediction of room temperature antiferromagnetism in V_2CT_2 (T = Cl, Br, I) MXenes"

by Kan Luo, Xianghua Kong, Shiyu Du and Hong Guo

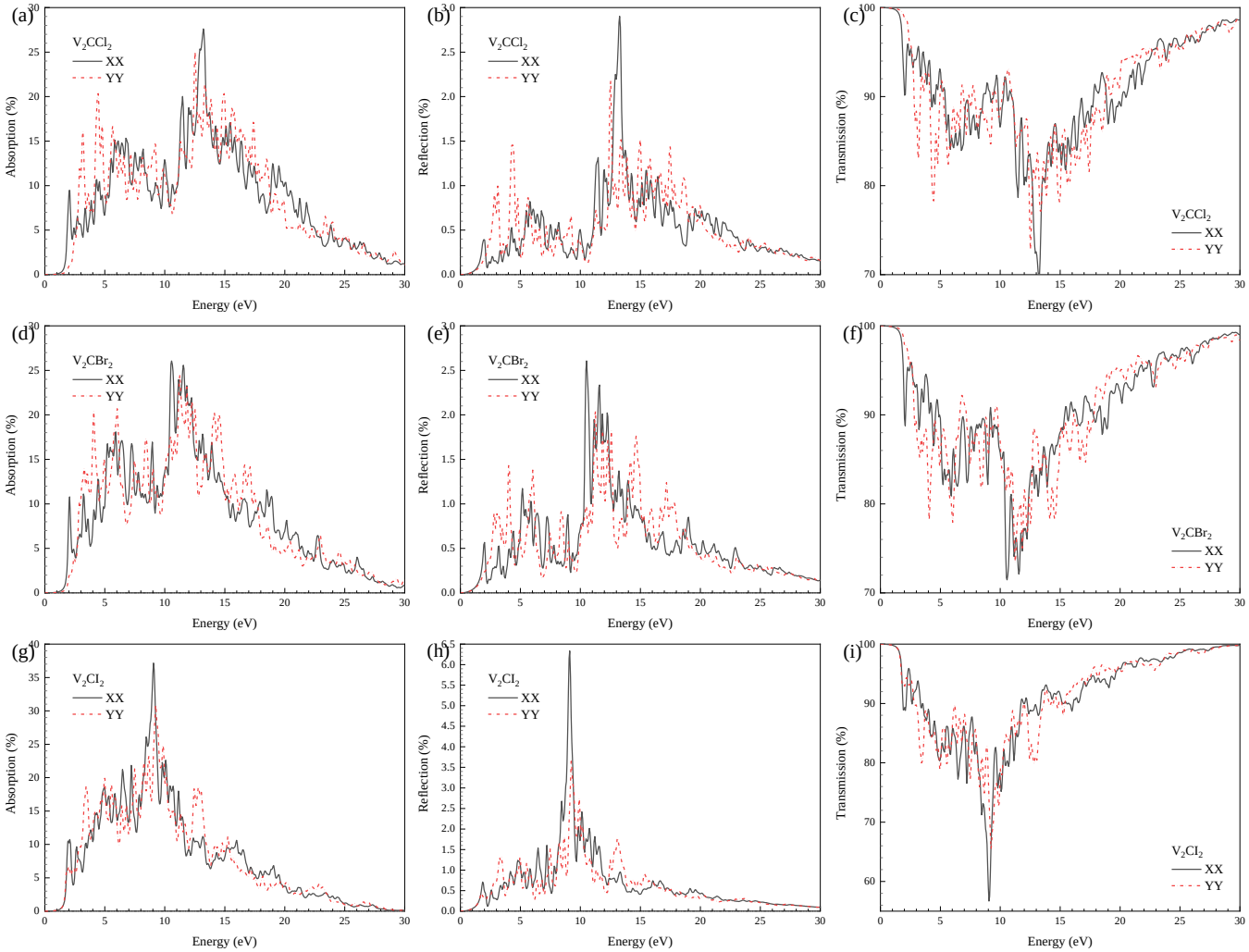

FIG. S5: The absorption, reflection, and transmission spectra for V_2CT_2 (T = Cl, Br, I).

Supplementary Material for "Prediction of room temperature antiferromagnetism in V_2CT_2 (T = Cl, Br, I) MXenes"

by Kan Luo, Xianghua Kong, Shiyu Du and Hong Guo

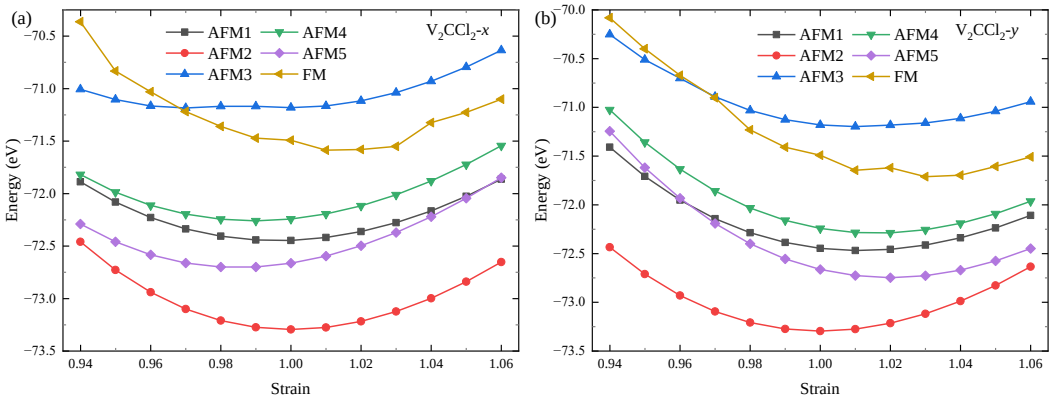

FIG. S6: Total energy variation under x or y-axis stain for the V_2CCl_2.

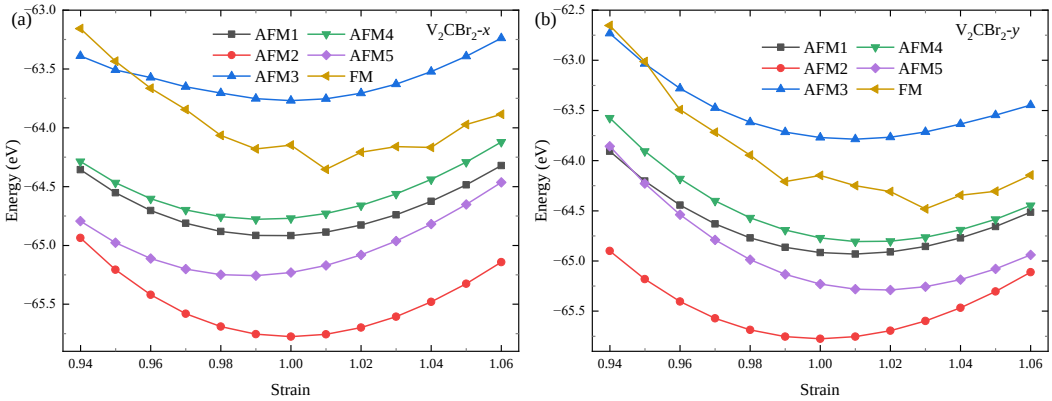

FIG. S7: Total energy variation under x or y-axis stain for the V_2CBr_2.

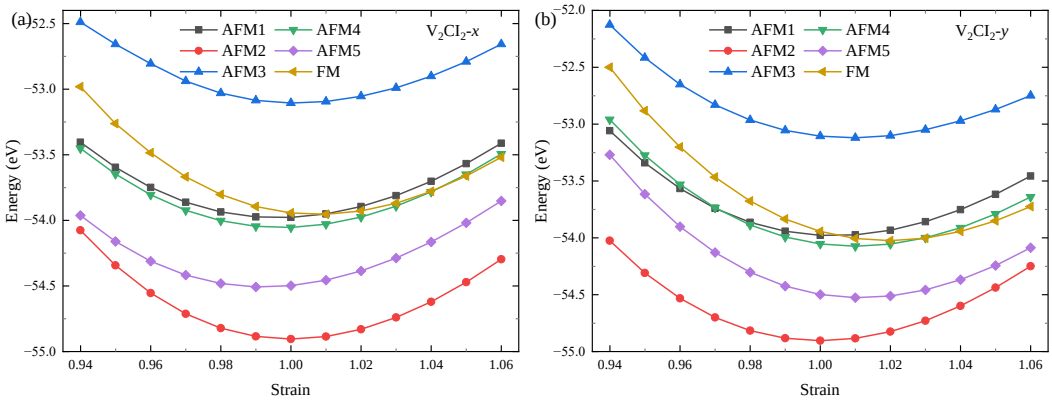

FIG. S8: Total energy variation under x or y-axis stain for the V_2CI_2.